

THE ERA OF REIONIZATION

Piero Madau ¹

RESUMEN

El resumen será traducido al español por los editores. In popular cold dark matter cosmological scenarios, stars may have first appeared in significant numbers around a redshift of 10 or so, as the gas within protogalactic halos with virial temperatures $T_{\text{vir}} \gtrsim 10^{4.3}$ K (corresponding to masses comparable to those of present-day dwarf ellipticals) cooled rapidly due to atomic processes and fragmented. It is this ‘second generation’ of subgalactic stellar systems, aided perhaps by an early population of accreting black holes in their nuclei, which may have generated the ultraviolet radiation and mechanical energy that ended the cosmic “dark ages” and reheated and reionized most of the hydrogen in the universe by a redshift of 6. The detailed history of the universe during and soon after these crucial formative stages depends on the power-spectrum of density fluctuations on small scales and on a complex network of poorly understood ‘feedback’ mechanisms, and is one of the missing link in galaxy formation and evolution studies. The astrophysics of the epoch of first light is recorded in the thermal state, ionization degree, and chemical composition of the intergalactic medium, the main repository of baryons at high redshifts.

ABSTRACT

In popular cold dark matter cosmological scenarios, stars may have first appeared in significant numbers around a redshift of 10 or so, as the gas within protogalactic halos with virial temperatures $T_{\text{vir}} \gtrsim 10^{4.3}$ K (corresponding to masses comparable to those of present-day dwarf ellipticals) cooled rapidly due to atomic processes and fragmented. It is this ‘second generation’ of subgalactic stellar systems, aided perhaps by an early population of accreting black holes in their nuclei, which may have generated the ultraviolet radiation and mechanical energy that ended the cosmic “dark ages” and reheated and reionized most of the hydrogen in the universe by a redshift of 6. The detailed history of the universe during and soon after these crucial formative stages depends on the power-spectrum of density fluctuations on small scales and on a complex network of poorly understood ‘feedback’ mechanisms, and is one of the missing link in galaxy formation and evolution studies. The astrophysics of the epoch of first light is recorded in the thermal state, ionization degree, and chemical composition of the intergalactic medium, the main repository of baryons at high redshifts.

Key Words: COSMOLOGY — DIFFUSE RADIATION — INTERGALACTIC MEDIUM

1. INTRODUCTION

At epochs corresponding to $z \sim 1000$ the intergalactic medium (IGM) is expected to recombine and remain neutral until sources of radiation and heat develop that are capable of reionizing it. The detection of transmitted flux shortward of the Ly α wavelength in the spectra of sources at $z \gtrsim 5$ implies that the hydrogen component of this IGM was ionized at even higher redshifts. The increasing thickening of the Ly α forest recently measured in the spectra of SDSS $z \sim 6$ quasars (Becker et al.2001; Djorgovski et al.2001) may be the signature of the trailing edge of the cosmic reionization epoch. It is clear that substantial sources of ultraviolet photons and mechanical energy, like young star-forming galaxies, were already present back then. The reionization of

intergalactic hydrogen at $z \gtrsim 6$ is unlikely to have been accomplished by quasi-stellar sources: the observed dearth of luminous optical and radio-selected QSOs at $z > 3$ (Shaver et al.1996; Fan et al.2001), together with the detection of substantial Lyman-continuum flux in a composite spectrum of Lyman-break galaxies at $\langle z \rangle = 3.4$ (Steidel et al. 2001), both may support the idea that massive stars in galactic and subgalactic systems – rather than quasars – reionized the hydrogen component of the IGM when the universe was less than 5% of its current age, and dominate the 1 ryd metagalactic flux at all redshifts greater than 3. An episode of pregalactic star formation may also provide a possible explanation for the widespread existence of heavy elements (like carbon, oxygen, and silicon) in the IGM. There is mounting evidence that the double reionization of helium may have occurred later, at a redshift of 3 or so (see Kriss

¹Department of Astronomy and Astrophysics, University of California, Santa Cruz, CA 95064, USA.

et al. 2001, and references therein): this is likely due to the integrated radiation emitted above 4 ryd by QSOs.

Establishing what ended the dark ages and when is important for determining the impact of cosmological reionization and reheating on several key cosmological issues, from the role reionization plays in allowing protogalactic objects to cool and make stars, to determining the thermal state of baryons at high redshifts and the small-scale structure in the temperature fluctuations of the cosmic microwave background. Conversely, probing the reionization epoch may provide a means for constraining competing models for the formation of cosmic structures: for example, popular modifications of the CDM paradigm that attempt to improve over CDM by suppressing the primordial power-spectrum on small scales, like warm dark matter (WDM), are known to reduce the number of collapsed halos at high redshifts and make it more difficult to reionize the universe (Barkana et al.2001). In this talk I will summarize some recent theoretical developments in understanding the astrophysics of the epoch of first light and the impact that some of the earliest generations of stars, galaxies, and black holes in the universe may have had on the IGM.

2. REIONIZATION BY MASSIVE STARS

In a cold dark matter (CDM) universe, structure formation is a hierarchical process in which non linear, massive structures grow via the merger of smaller initial units. Large numbers of low-mass galaxy halos are expected to form at early times in these popular theories, leading to an era of reionization, reheating, and chemical enrichment. Most models predict that intergalactic hydrogen was reionized by an early generation of stars or accreting black holes at $z = 7 - 15$. One should note, however, that while numerical N-body+hydrodynamical simulations have convincingly shown that the IGM does fragment into structures at early times in CDM cosmogonies (e.g. Cen et al.1994; Zhang et al.1995; Hernquist et al.1996), the same simulations are much less able to predict the efficiency with which the first gravitationally collapsed objects lit up the universe at the end of the dark age.

The scenario that has received the most theoretical studies is one where hydrogen is photoionized by the UV radiation emitted either by quasars or by stars with masses $\gtrsim 10 M_{\odot}$ (e.g. Shapiro & Giroux 1987; Haiman & Loeb 1998; Madau et al.1999; Chiu & Ostriker 2000; Ciardi et al.2000), rather than ionized by collisions with electrons heated up by, e.g.

supernova-driven winds from early pregalactic objects. In the former case a high degree of ionization requires about $13.6 \times (1 + t/\bar{t}_{\text{rec}})$ eV per hydrogen atom, where \bar{t}_{rec} is the volume-averaged hydrogen recombination timescale, t/\bar{t}_{rec} being much greater than unity already at $z \sim 10$ according to numerical simulations. Collisional ionization to a neutral fraction of only a few parts in 10^5 requires a comparable energy input, i. e. an IGM temperature close to 10^5 K or about 25 eV per atom.

Massive stars will deposit both radiative and mechanical energy into the interstellar medium of protogalaxies. A complex network of ‘feedback’ mechanisms is likely at work in these systems, as the gas in shallow potential is more easily blown away (Dekel & Silk 1986; Tegmark et al.1993; Mac Low & Ferrara 1999; Mori et al. 2002) thereby quenching star formation. Furthermore, as the blastwaves produced by supernova explosions reheat the surrounding intergalactic gas and enrich it with newly formed heavy elements (see below), they can inhibit the formation of surrounding low-mass galaxies due to ‘baryonic stripping’ (Scannapieco et al.2002). It is therefore difficult to establish whether an early input of mechanical energy will actually play a major role in determining the thermal and ionization state of the IGM on large scales. What can be easily shown is that, during the evolution of a ‘typical’ stellar population, more energy is lost in ultraviolet radiation than in mechanical form. This is because in nuclear burning from zero to solar metallicity ($Z_{\odot} = 0.02$), the energy radiated per baryon is $0.02 \times 0.007 \times m_{\text{H}} c^2$, with about one third of it going into H-ionizing photons. The same massive stars that dominate the UV light also explode as supernovae (SNe), returning most of the metals to the interstellar medium and injecting about 10^{51} ergs per event in kinetic energy. For a Salpeter initial mass function (IMF), one has about one SN every 150 M_{\odot} of baryons that forms stars. The mass fraction in mechanical energy is then approximately 4×10^{-6} , ten times lower than the fraction released in photons above 1 ryd.

The relative importance of photoionization versus shock ionization will depend, however, on the efficiency with which radiation and mechanical energy actually escape into the IGM. Consider, for example, the case of an early generation of subgalactic systems collapsing at redshift 9 from $2\text{-}\sigma$ fluctuations. At these epochs their dark matter halos would have virial radii $r_{\text{vir}} = 0.75 h^{-1}$ Kpc and circular velocities $V_c(r_{\text{vir}}) = 25 \text{ km s}^{-1}$, corresponding in top-hat spherical collapse to a virial temperature $T_{\text{vir}} = 0.5 \mu m_p V_c^2 / k \approx 10^{4.3}$ K and halo mass

$M = 0.1V_c^3/GH \approx 10^8 h^{-1} M_\odot$.² Halos in this mass range are characterized by very short dynamical timescales (and even shorter gas cooling times due to atomic hydrogen) and may therefore form stars in a rapid but intense burst before SN ‘feed-back’ quenches further star formation. For a star formation efficiency of $f = 0.1$, $\Omega_b h^2 = 0.02^3$, $h = 0.5$, and a Salpeter IMF, the explosive output of 10,000 SNe will inject an energy $E_0 \approx 10^{55}$ ergs. This is roughly a hundred times higher than the gas binding energy: a significant fraction of the halo gas will then be lifted out of the potential well (‘blow-away’) and shock the intergalactic medium (Madau et al.2001). If the explosion occurs at cosmic time $t = 4 \times 10^8$ yr (corresponding in the adopted cosmology to $z = 9$), at time $\Delta t = 0.4t$ after the event it is a good approximation to treat the cosmological blast wave as adiabatic, with proper radius given by the standard Sedov–Taylor self-similar solution,

$$R_s \approx \left(\frac{12\pi G \eta E_0}{\Omega_b} \right)^{1/5} t^{2/5} \Delta t^{2/5} \approx 17 \text{ kpc}. \quad (1)$$

Here $\eta \approx 0.3$ is the fraction of the available SN energy that is converted into kinetic energy of the blown-away material (Mori et al.2002). At this instant the shock velocity relative to the Hubble flow is

$$v_s \approx 2R_s/5\Delta t \approx 40 \text{ km s}^{-1}, \quad (2)$$

lower than the escape velocity from the halo center. The gas temperature just behind the shock front is $T_s = 3\mu m_p v_s^2/16k \gtrsim 10^{4.3}$ K, enough to ionize all incoming intergalactic hydrogen. At these redshifts, it is the onset of Compton cooling off cosmic microwave background photons that ends the adiabatic stage of blast wave propagation; the shell then enters the snowplough phase and is finally confined by the IGM pressure. According to the Press–Schechter formalism, the comoving abundance of collapsed dark halos with mass $M = 10^8 h^{-1} M_\odot$ at $z = 9$ is $dn/d\ln M \sim 80 h^3 \text{ Mpc}^{-3}$, corresponding to a mean proper distance between neighboring halos of $\sim 15 h^{-1} \text{ kpc}$. With the assumed star formation efficiency, only a small fraction, about 4 percent, of the total stellar mass inferred today (Fukugita et al.1998) would actually form at these early epochs. Still, our simple analysis shows that the blast waves from such a population of pregalactic objects could drive vast portions of the IGM to a significantly

higher adiabat, $T_{\text{IGM}} \sim 10^5$ K, than expected from photoionization, so as to ‘choke off’ the collapse of further $M \lesssim 10^9 h^{-1} M_\odot$ systems by raising the cosmological Jeans mass. In this sense the process may be self-regulating.

The thermal history of expanding intergalactic primordial gas at the mean density is plotted in Figure 1 as a function of redshift for a number of illustrative cases. The code we have used includes the relevant cooling and heating processes and follows the non-equilibrium evolution of hydrogen and helium ionic species in a cosmological context.

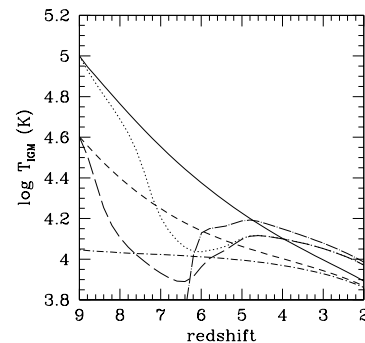


Fig. 1: Thermal history of intergalactic gas at the mean density in an Einstein–de Sitter universe with $\Omega_b h^2 = 0.02$ and $h = 0.5$. *Short dash-dotted line*: temperature evolution when the only heating source is a constant ultraviolet (CUV) background of intensity $10^{-22} \text{ ergs cm}^{-2} \text{ s}^{-1} \text{ Hz}^{-1} \text{ sr}^{-1}$ at 1 Ryd and power-law spectrum with energy slope $\alpha = 1$. *Long dash-dotted line*: same for the time-dependent quasar ionizing background as computed by Haardt & Madau (1996; HM). *Short-dashed line*: heating due to a CUV background but with an initial temperature of 4×10^4 K at $z = 9$ as expected from an early era of pregalactic outflows. *Long-dashed line*: same but for a HM background. *Solid line*: heating due to a CUV background but with an initial temperature of 10^5 K at $z = 9$. *Dotted line*: same but for a HM background.

The gas is allowed to interact with the CMB through Compton cooling and either with a time-dependent QSO ionizing background as computed by Haardt & Madau (1996) or with a time-independent metagalactic flux of intensity $10^{-22} \text{ ergs cm}^{-2} \text{ s}^{-1} \text{ Hz}^{-1} \text{ sr}^{-1}$ at 1 Ryd (and power-law spectrum with energy slope $\alpha = 1$). The temperature of the medium at $z = 9$ – where we start our integration – has been either computed self-consistently from photoheating or fixed to be in the range $10^{4.6} - 10^5$ K expected from SN-driven bubbles with significant filling factors (see below). The various curves show that the temperature of the IGM at $z = 3 - 4$ will retain little memory of an early era of pregalactic outflows and preheating, and be consistent with that expected from photoionization.

²This assumes an Einstein–de Sitter universe with Hubble constant $H_0 = 100 h \text{ km s}^{-1} \text{ Mpc}^{-1}$.

³Here Ω_b is the baryon density parameter, and $f\Omega_b$ is the fraction of halo mass converted into stars.

3. FEEDBACK AND PREGALACTIC ENRICHMENT

Understanding the origin of the chemical elements, following the increase in their abundances with cosmic time, and uncovering the processes responsible for distributing the products of stellar nucleosynthesis over very large distances are all key aspects of the evolution of gaseous matter in the universe. One of the major discoveries with *Keck* concerning the IGM has been the identification of metal absorption lines associated with many of the Ly α forest systems. The detection of measurable C IV and Si IV absorption lines in clouds with H I column densities as low as $10^{14.5} \text{ cm}^{-2}$ implies a minimum universal metallicity relative to solar in the range $[-3.2]$ to $[-2.5]$ at $z \sim 3$ (Songaila 1997). There is no indication in the data of a turnover in the C IV column density distribution down to $N_{\text{CIV}} \lesssim 10^{11.7} \text{ cm}^{-2}$ ($N_{\text{HI}} \lesssim 10^{14.2} \text{ cm}^{-2}$, Ellison et al.2000).

From a theoretical perspective, it is unclear whether the existence of heavy elements in the IGM at $z = 3 - 3.5$ points to an early ($z > 6$) enrichment epoch by low-mass subgalactic systems (Madau et al.2001), or is rather due to late pollution by the population of star-forming galaxies known to be already in place at $z = 3$. The Press-Schechter theory for the evolving mass function of dark matter halos predicts a power-law dependence, $dN/d \ln m \propto m^{(n_{\text{eff}}-3)/6}$, where n_{eff} is the effective slope of the CDM power spectrum, $n_{\text{eff}} \approx -2.5$ on subgalactic scales. As hot, metal-enriched gas from SN-driven winds escapes its host halo, shocks the IGM, and eventually forms a blast wave, it sweeps a region of intergalactic space the volume of which increases with the $3/5$ power of the injected energy E_0 (in the adiabatic Sedov-Taylor phase). The total fractional volume or porosity, Q , filled by these ‘metal bubbles’ per unit explosive energy density $E_0 dN/d \ln m$ is then $Q \propto E_0^{3/5} dN/d \ln m \propto (dN/d \ln m)^{2/5} \propto m^{-11/30}$. Within this simple scenario it is the star-forming objects with the smallest masses which will arguably be the most efficient pollutant of the IGM on large scales. Metal-enriched material from SN ejecta may be far more easily accelerated to escape velocities in the shallow potential wells of subgalactic systems at $z > 6$. Late enrichment may also encounter problems in explaining the kinematic quiescence of C IV lines; the observed small scale properties of the IGM at $z \sim 3$ appear consistent with C IV absorbers being the result of ancient pregalactic outflows (Rauch et al.2001). According to numerical hydrodynamics simulations of structure formation in the IGM, the

metals associated with $\log N_{\text{HI}} \lesssim 14$ filaments fill a fraction $\gtrsim 5\%$ of intergalactic space, and are therefore far away from the high overdensity peaks where galaxies form, gas cools, and star formation takes place. Their chemical enrichment may then reflect more uniform (i.e. ‘early’) rather than in-situ (i.e. ‘late’) metal pollution. The case for pregalactic enrichment may have been recently strengthened by the observation of an invariant C IV column density distribution throughout the redshift range $2 < z < 5$ (Songaila 2001).

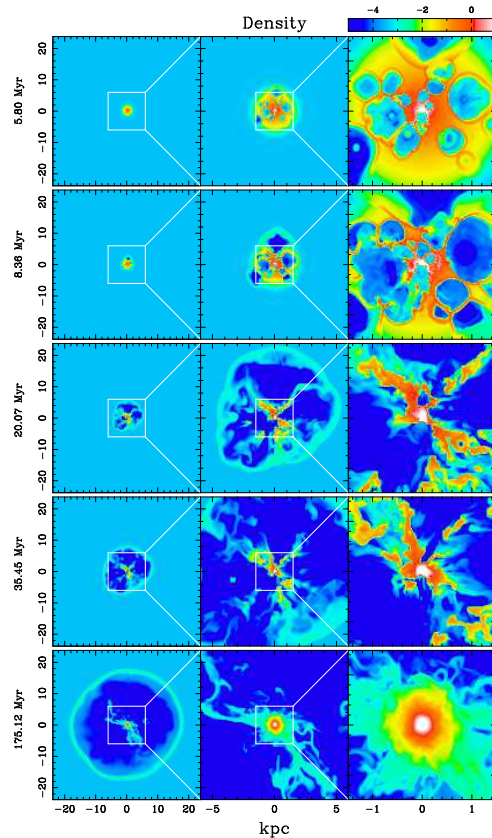


Fig. 2: Snapshots of the logarithmic number density of the gas at five different elapsed times for our Case 1 simulation run. The three panels in each row show the spatial density distribution in the $X - Y$ plane on the nested grids. The three columns in each figure depict the time evolution from about 6 Myr to up to 180 Myr. Along a given row, the leftmost panel refers to grid L5 (linear size 48 kpc), the central one to grid L3 (linear size 12 kpc), and the rightmost panel refers to the grid L1 (linear size 3 kpc). The density range is $-5 \leq \log (n/\text{cm}^{-3}) \leq 1$. The halo gas is assumed to be initially in hydrostatic equilibrium and non self-gravitating. (From Mori et al.2002.)

To simulate the process of blow-away we have developed a 3D Eulerian code that solves the hydro-

dynamic equations for a perfect fluid in Cartesian geometry. To deal with very different length scales in our simulation we have adopted a ‘nested grid method’ with six levels of fixed Cartesian grids. The grids are connected by the transfer of conserved variables, and are centered within each other, with the finest covering the whole galaxy halo. Since the cell number is the same ($128 \times 128 \times 128$) for every level Ln ($n = 1, 2, \dots, 6$), the minimum resolved scale is about 22 pc and the size of the coarsest grid is 96 kpc. Thus, the scheme has a wide dynamic range in the space dimension.

The results of a numerical simulation (run on massive parallel supercomputers at the Center for Computational Physics, Tsukuba University) are depicted in Figure 2. In this run about 10,000 SNe explode in a high redshift protohalo (corresponding to a star formation efficiency of about 10% for a Salpeter IMF). Our algorithm for simulating SN feedback improves upon previous treatments in several ways. OB associations are distributed as a function of gas density according to a Schmidt-type law ($\propto \rho^\alpha$) using a Monte-Carlo procedure. After a main sequence lifetime, all stars more massive than $8 M_\odot$ explode instantaneously injecting an energy of 10^{51} ergs, and their outer layers are blown out leaving a compact remnant of $1.4 M_\odot$. Therefore SNe inject energy (assumed in pure thermal form) and mass into the interstellar medium: these are supplied to a sphere corresponding to the radius of a SN remnant in a uniform ambient medium of density n and in the adiabatic Sedov-Taylor phase; the expansion velocity is also self-consistently calculated from such solution. The gas then starts cooling immediately according to the adopted gas cooling function. While the time-step Δt is controlled by the Courant condition, if there are more than two SN events in a OB association we decrease Δt until only one explosion per association occurs during the time-step.

Snapshots of the gas density distribution in a planar slice of the nested grids are shown for an extended stellar distribution case ($\alpha = 1$). After a few Myr from the beginning of the simulation the most massive stars explode as SNe and produce expanding hot bubbles surrounded by a cooling dense ($n \approx 1 \text{ cm}^{-3}$) shell. As the evolution continues, a coherent and increasingly spherical shell expanding into the IGM is eventually formed. The shell contains a large fraction of the halo gas that has been swept-up during the evolution. The final bottom row of the simulation figure shows the final stages of the evolution: the shell is now nearly spherically symmetric, its interior being filled with warm ($T \lesssim 10^6 \text{ K}$) gas

at a very low density $n \lesssim 10^{-4} \text{ cm}^{-3}$, i.e. slightly below the mean value for the IGM. At the end of the simulations, the shell is still sweeping out IGM material; its radius and velocity are 21 kpc and 26 km sec^{-1} at $t = 250 \text{ Myr}$. Using momentum conservation one can estimate the final radius of the shell to be close to 25 kpc. This is about 17 times the virial radius of the halo!

It is clear then that SN-driven pregalactic outflows may be an efficient mechanism for spreading metals around. The collective explosive output of about ten thousands SNe per $M \gtrsim 10^8 h^{-1} M_\odot$ halo at these early epochs could then pollute the entire intergalactic space to a mean metallicity $\langle Z \rangle = \Omega_Z / \Omega_b \gtrsim 0.003$ (comparable to the levels observed in the Ly α forest at $z \approx 3$) without much perturbing the IGM hydrodynamically, i.e. producing large variations of the baryons relative to the dark matter. The significance of these results goes well beyond early metal enrichment. This is because, since the cooling time of collisionally ionized high density gas in small halos at high redshifts is much shorter than the then Hubble time, virtually all baryons are predicted to sink to the centers of these halos in the absence of any countervailing effect (White & Rees 1978). Efficient feedback is then necessary in hierarchical clustering scenarios to avoid this ‘cooling catastrophe’, i.e. to prevent too many baryons from turning into stars as soon as the first levels of the hierarchy collapse. The required reduction of the stellar birthrate in halos with low circular velocities may naturally result from the heating and expulsion of material due to OB stellar winds and repeated SN explosions from the first burst of star formation.

4. PROBING THE EPOCH OF FIRST LIGHT AT 21-CM

Prior to the epoch of full reionization, the intergalactic medium and gravitationally collapsed systems may be detectable in emission or absorption against the CMB at the frequency corresponding to the redshifted 21-cm line (associated with the spin-flip transition from the triplet to the singlet state of neutral hydrogen.) In general, 21-cm spectral features are expected to display angular structure as well as structure in redshift space due to inhomogeneities in the gas density field, hydrogen ionized fraction, and spin temperature. Several different signatures have been investigated in the recent literature: (a) the fluctuations in the redshifted 21-cm emission induced by the gas density inhomogeneities that develop at early times in CDM-dominated cosmologies (Madau et al.1997; Tozzi et al.2000) and

by virialized “minihalos” with $T_{\text{vir}} < 10^4$ K (Iliev et al.2002); (b) the sharp absorption feature in the radio sky due to the rapid rise of the Ly α continuum background that marks the birth of the first UV sources in the universe (Shaver et al.1999); (c) the 21-cm narrow lines generated in absorption against very high-redshift radio sources by the neutral IGM (Carilli et al.2002) and by intervening minihalos and protogalactic disks (Furlanetto & Loeb 2002).

A quick summary of the physics of 21-cm radiation will illustrate the basic ideas and unresolved issues behind these studies. The emission or absorption of 21-cm photons from a neutral IGM is governed by the hydrogen spin temperature T_S defined by $n_1/n_0 = 3 \exp(-T_*/T_S)$, where n_0 and n_1 are the singlet and triplet $n = 1$ hyperfine levels and $k_B T_* = 5.9 \times 10^{-6}$ eV is the energy of the 21-cm transition. In the presence of only the CMB radiation with $T_{\text{CMB}} = 2.73(1+z)$ K, the spin states will reach thermal equilibrium with the CMB on a timescale of $T_*/(T_{\text{CMB}} A_{10}) \approx 3 \times 10^5 (1+z)^{-1}$ yr ($A_{10} = 2.9 \times 10^{-15} \text{ s}^{-1}$ is the spontaneous decay rate of the hyperfine transition of atomic hydrogen), and intergalactic H I will produce neither an absorption nor an emission signature. A mechanism is required that decouples T_S and T_{CMB} , e.g. by coupling the spin temperature instead to the kinetic temperature T_K of the gas itself. Two mechanisms are available, collisions between hydrogen atoms (Purcell & Field 1956) and scattering by Ly α photons (Field 1958). The collision-induced coupling between the spin and kinetic temperatures is dominated by the spin-exchange process between the colliding hydrogen atoms. The rate, however, is too small for realistic IGM densities at the redshifts of interest, although collisions may be important in dense regions with $\delta\rho/\rho \gtrsim 30[(1+z)/10]^{-2}$, like virialized minihalos.

In the low density IGM, the dominant mechanism is the scattering of continuum UV photons redshifted by the Hubble expansion into local Ly α photons. The many scatterings mix the hyperfine levels of neutral hydrogen in its ground state via intermediate transitions to the $2p$ state, the Wouthuysen-Field process. As the neutral IGM is highly opaque to resonant scattering, the shape of the continuum radiation spectrum near Ly α will follow a Boltzmann distribution with a temperature given by the kinetic temperature of the IGM (Field 1959). In this case the spin temperature of neutral hydrogen is a weighted mean between the matter and CMB temperatures. There exists then a critical value of the background flux of Ly α photons which, if greatly ex-

ceeded, would drive the spin temperature away from T_{CMB} .

While the microphysics is well understood, our understanding of the astrophysics of 21-cm tomography is still poor. In Tozzi et al.(2000) we used N-body cosmological simulations and, assuming a fully neutral medium with $T_S \gg T_{\text{CMB}}$, showed that prior to reionization the same network of sheets and filaments (the ‘cosmic web’) that gives rise to the Ly α forest at $z \sim 3$ should lead to fluctuations in the 21-cm brightness temperature at higher redshifts (Figure 3). At 150 MHz ($z = 8.5$), for observations with a bandwidth of 1 MHz, the root mean square fluctuations should be ~ 10 mK at 1', decreasing with scale. Because of the smoothness of the CMB sky, fluctuations in the 21-cm radiation will dominate the CMB fluctuations by about 2 orders of magnitude on arcmin scales. The search at 21-cm for the epoch of first light has become one of the main science drivers of the *LOW Frequency ARray* (*LOFAR*; see <http://www.astron.nl/lofar/science/>). While remaining an extremely challenging project due to foreground contamination from extragalactic radio sources (Di Matteo et al.2002), the detection and imaging of these small-scale structures with *LOFAR* is a tantalizing possibility within range of the thermal noise of the array.

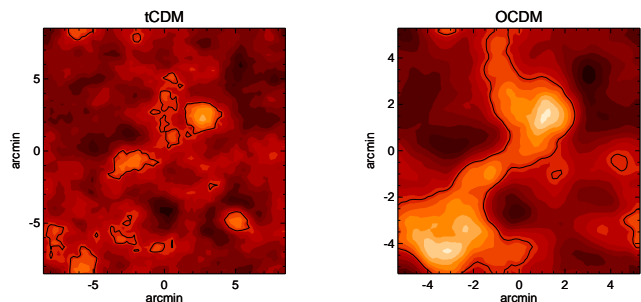


Fig. 3: *Left*: Radio map of redshifted 21-cm emission against the CMB in a ‘tilted’ CDM (tCDM) cosmology at $z = 8.5$. Here a collisionless N -body simulation with 64^3 particles has been performed with Hydra (Couchman et al.1995). The simulation box size is $20h^{-1}$ comoving Mpc, corresponding to 17 (11) arcmin in tCDM (OCDM). The baryons are assumed to trace the dark matter distribution without any biasing, the spin temperature to be much greater than the temperature of the CMB everywhere, and the gas to be fully neutral. The point spread function of the synthesized telescope beam is a spherical top-hat with a width of 2 arcmin. The frequency window is 1 MHz around a central frequency of 150 MHz. The contour levels outline regions with signal greater than $4 \mu\text{Jy}$ per beam. *Right*: Same for an open cosmology (OCDM). Since the growth of density fluctuations ceases early on in an open universe (and the power spectrum is normalized to the abundance of clusters today), the signal at a given angular

size is much larger in OCDM than in Λ CDM at these early epochs. (From Tozzi et al.2000.)

On the theoretical side, there are several effects that need to be examined further. As mentioned above, it is the presence of a sufficient flux of Ly α photons which renders the neutral IGM ‘visible’. Without heating sources, the adiabatic expansion of the universe will lower the kinetic temperature of the gas well below that of the CMB, and the IGM will be detectable through its absorption. If there are sources of radiation that preheat the IGM, it may be possible to detect it in emission instead. The energetic demand for heating the IGM above the CMB temperature is meager, only ~ 0.004 eV per particle at $z \sim 10$. Consequently, even relatively inefficient heating mechanisms may be important warming sources well before the universe was actually reionized. Perhaps more importantly, prior to full reionization the IGM will be a mixture of neutral, partially ionized, and fully ionized structures: low-density regions will be fully ionized first, followed by regions with higher and higher densities. Radio maps at 21 (1+z) cm will show a patchwork of emission/absorption signals from H I zones modulated by H II regions where no signal is detectable against the CMB. It is the early generation of stars likely responsible for reionization which will also generate a background radiation field of photons with energies between 10.2–13.6 eV to which the IGM is transparent. As each of these photons gets redshifted, it ultimately reaches the Ly α transition energy of 10.2 eV, scatters resonantly off neutral hydrogen, and mixes the hyperfine levels. The observability of the pre-reionization IGM depends in this case on the UV spectrum of the first stars, i.e. on the number of Ly α continuum photons emitted per H-ionizing photon.

The integrated UV spectrum of a stellar population is characterized by a strong break at the Lyman edge whose size depends on age, initial mass function, and star formation history. In Figure 4 we have therefore normalized the Ly α rate to the rate of emission of hydrogen-ionizing photons; after integrating over the stellar age, τ , a starburst is characterized by a ratio $N_\alpha/N_{\text{ion}} \approx 22 (\tau/0.1 \text{ Gyr})^{0.22}$ (Scalo IMF), about three times higher than the constant SFR case (this is because of the shorter lifetime of the massive stars that produce 1 ryd radiation). It is possible that the startburst mode may be more relevant for the galaxies responsible for reionization, as stellar winds and supernovae can easily expell the gas out of the shallow potential wells of low mass ha-

los, after the first burst of star formation occurs. In this case the escape fraction might be low until the gas is expelled, and as Figure 4 indicates this would contribute to an even stronger Ly α continuum emission per ionizing flux.

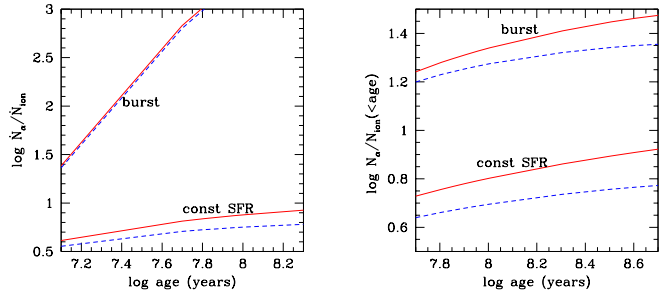


Fig. 4: *Left:* Continuum Ly α photon emission rate \dot{N}_α (s^{-1}) versus age (in years) for a stellar population with a Salpeter IMF (*dashed lines*) and a Scalo IMF (*solid lines*). Upper curves assume an instantaneous burst of star formation, lower curves a constant star formation rate. The rate of production of Ly α photons has been normalized to the rate of emission of hydrogen-ionizing photons, \dot{N}_{ion} . The population synthesis values have been computed for low metallicities ($Z = 0.02 Z_\odot$), and are based on an update of Bruzual & Charlot’s (1993) libraries. *Right:* Same after integration over the age of the stellar population.

5. PHOTON CONSUMPTION IN MINIHALOS DURING COSMOLOGICAL REIONIZATION

The process of reionization has recently received much theoretical attention, and has been studied by several authors using semi-analytic models (e.g. Meiksin & Madau 1993; Shapiro et al.1994; Haiman & Loeb 1997, 1998; Benson et al.2001) and three-dimensional numerical simulations (Gnedin 2000). In general, these works aim to follow the time evolution of the filling factor of ionized (H II) regions, based on some input prescriptions for the emissivity and spectra of the ionizing sources.

More recent works have focused on the increased rate of recombinations in a clumpy medium relative to a homogeneous one, i.e. when $\langle \rho^2 \rangle > \langle \rho \rangle^2$ (Ciardi et al. 2000; Benson et al.2001; Chiu & Ostriker 2000; Gnedin 2000; Madau et al.1999). These studies have left significant uncertainties on the details of how reionization proceeds in an inhomogeneous medium. Since the ionizing sources are embedded in dense regions, one might expect that these dense regions are ionized first, before the radiation escapes to ionize the low-density IGM. Alternatively, most of the radiation might escape from the local, dense regions along low column density lines of sight. In this

case, the underdense ‘voids’ are ionized first, with the ionization of the denser filaments and halos lagging behind (Miralda-Escudé et al. 2000).

At the earliest epochs of structure formation in CDM cosmologies the smallest nonlinear objects are the numerous small halos that condense with virial temperatures between the cosmological Jean temperature and $\sim 10^4$ K. Such “minihalos” are not yet fully resolved nor is the process of their photoevaporation captured in large-scale three-dimensional cosmological simulations.⁴ In Haiman et al.(2001) we have used semi-analytic methods combined with three-dimensional numerical simulations of individual photoevaporating minihalos to (1) quantify the importance of high-redshift minihalos as sinks of ionizing photons; and (2) assess whether by extrapolating to early times the known population of galaxies and quasars a sufficient number of UV photons are produced for hydrogen reionization. If reionization occurs at sufficiently high redshifts ($z_r \gtrsim 20$), the intergalactic medium is heated to $\sim 10^4$ K and most minihalos never form.

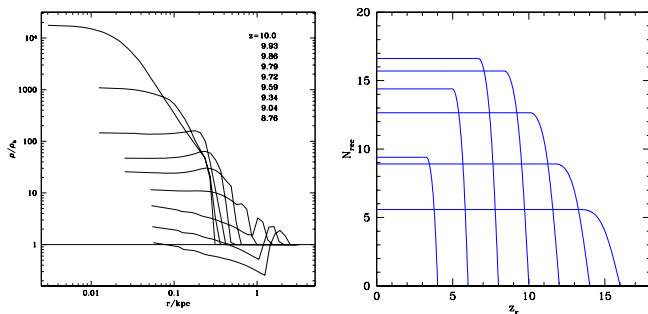


Fig. 5: *Left*: The evolution of the density profile of a minihalo with mass $10^6 M_\odot$, illuminated by a UV background flux at $z = 10$. The hydrogen photoionization rate is assumed to be uniform on the grid, i.e. we do not solve radiative transfer. Photoevaporation occurs very rapidly, with most recombinations occurring within a sound-crossing time. The figure reveals that by $z = 9.5$ the density contrast is everywhere reduced below $\delta \lesssim 10$. *Right*: Total number of recombinations inside minihalos, following sudden reionization at redshift z_r . Recombinations are shown per background hydrogen atom. In the earliest stages of reionization, minihalos dominate the average gas clumping in the universe, and can therefore dominate the total recombination rate. (From Haiman et al.2001.)

On the other hand, if $z_r \lesssim 20$ as it now appears

⁴Photoionization by either a nearby external UV source, or by the smooth cosmic UV background radiation after the reionization epoch will heat the gas inside a minihalo to a temperature $\approx 10^4$ K. By definition, the gas inside a minihalo is then no longer bound, leading to the photoevaporation of baryons out of their host halos (Shapiro, Raga & Mellema 1998; Barkana & Loeb 1999).

more likely, then a significant fraction ($\gtrsim 10\%$) of all baryons have already collapsed into minihalos, and are subsequently removed from the halos by photoevaporation as the ionizing background flux builds up (Figure 5). This process requires a significant budget of ionizing photons, about 10–20 of them per background hydrogen atom. This exceeds the production by a straightforward extrapolation back in time of known quasar and galaxy populations by a factor of up to ~ 10 and ~ 3 , respectively (Haiman et al.2001).

6. THE EARLIEST LUMINOUS SOURCES AND THE WING OF THE GUNN-PETERSON TROUGH

Prior to complete reionization at redshift z_r , sources of ultraviolet radiation will be seen behind a large column of intervening gas that is still neutral. In this case, because of scattering off the line-of-sight due to the diffuse neutral IGM, the spectrum of a source at $z_{\text{em}} > z_r$ should show the red damping wing of the Gunn-Peterson (1965) absorption trough at wavelengths longer than the local Ly α resonance, $\lambda_{\text{obs}} > \lambda_\alpha(1 + z_{\text{em}})$, where $\lambda_\alpha = c/\nu_\alpha = 1216 \text{ \AA}$. At $z_{\text{em}} \gtrsim 6$, this characteristic feature extends for more than 1500 km s^{-1} to the red of the resonance, and may significantly suppress the Ly α emission line in the spectra of the first generation of objects in the universe. Measuring the shape of the absorption profile of the damping wing could provide a determination of the density of the neutral IGM near the source (Miralda-Escudé 1998).

A number of authors (Madau & Rees 2000; Cen & Haiman 2000; Haiman 2002) have recently focused on the width of the red damping wing – related to the expected strength of the Ly α emission line – in the spectra of very distant QSOs and star-forming galaxies as a flag of the observation of the IGM before reionization. We have assessed, in particular, the impact of the photoionized, Mpc-size regions which will surround individual luminous sources of Lyman continuum radiation on the transmission of photons redward of the Ly α resonance, and shown that the damping wing of the Gunn-Peterson trough may nearly completely disappear because of the lack of neutral hydrogen in the vicinity of a bright QSO. The effect of this local photoionization is to greatly reduce the scattering opacity between the redshift of the quasar and the boundary of its H II region (Figure 6).

The detection of a strong Ly α emission line in the spectra of bright QSOs shining for $\gtrsim 10^7$ yr cannot then be used, by itself, as a constraint on the

reionization epoch. The first signs of an object radiating prior to the transition from a neutral to an ionized universe may be best searched for in the spectra of luminous sources with a small escape fraction of Lyman continuum photons into the IGM, or sources with a short duty cycle (like, e.g., gamma-ray bursts).

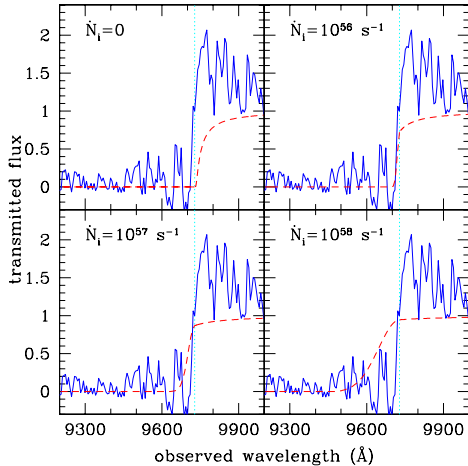


Fig. 6: The Keck/LRIS spectrum of the faint $z_{\text{em}} = 5.5$ quasar RD J0301117+002025 (Stern et al.2000), redshifted to $z_{\text{em}} = 7$. The dotted vertical lines indicate the expected wavelength of the Ly α resonance. Fluxes have arbitrary normalizations. The dashed curves show the transmission $\exp(-\tau_{\text{GP}})$ (where τ_{GP} is the Gunn-Peterson optical depth to resonant scattering) through a uniform IGM, assuming the QSO is being observed prior to the reionization epoch at $z_r = 6$. Four different cases are shown, as the rate of emission of Lyman continuum photons which ionize the IGM in the vicinity of the source is varied from $\dot{N}_i = 0$ to $\dot{N}_i = 10^{56}, 10^{57}$, and 10^{58} s^{-1} . The calculations assume a quasar lifetime of $t_s = 10^7 \text{ yr}$, a power-law spectrum of the form $f_\nu \propto \nu^{-\alpha}$ with $\alpha = 0.5$ near the hydrogen Lyman edge, a recombination timescale of $t_{\text{rec}} = 1.3 \text{ Gyr}$, an Einstein-de Sitter universe with $h = 0.5$, and a baryon density parameter $\Omega_B h^2 = 0.02$. (From Madau & Rees 2000.)

REFERENCES

- Barkana, R., Haiman, Z., & Ostriker, J. P. 2001, ApJ, 558, 482
- Barkana, R., & Loeb, A. 1999, ApJ, 523, 54
- Becker, R. H., et al.2001, AJ, 122, 2850
- Benson, A. J., Nusser, A., Sugiyama, N., & Lacey, C. G. 2001, MNRAS, 320, 153
- Bruzual, A. C., & Charlot, S. 1993, ApJ, 405, 538
- Carilli, C., Gnedin, N. Y., & Owen, F. 2002, ApJ, in press (astro-ph/0205169)
- Cen, R., & Haiman, Z. 2000, ApJ, 542, L75
- Cen, R., Miralda-Escudé, J., Ostriker, J. P., & Rauch, M. 1994, ApJ, 437, L9
- Chiu, W. A., & Ostriker, J. P. 2000, ApJ, 534, 507
- Ciardi, B., Ferrara, A., Governato, F., & Jenkins, A. 2000, MNRAS, 314, 611
- Couchman, H. M. P., Thomas, P. A., & Pearce, F. R. 1995, ApJ, 452, 797
- Dekel, A., & Silk, J. 1986, ApJ, 303, 39
- Di Matteo, T., Perna, R., Abel, T., & Rees, M. J. 2002, ApJ, in press (astr-ph/0109241)
- Djorgovski, S. G., Castro, S. M., Stern, D., & Mahabal, A. A. 2001, ApJ, 560, L5
- Ellison, S. L., Songaila, A., Schaye, J., & Pettini, M. 2000, AJ, 120, 1175
- Fan, X., et al.2001, AJ, 121, 54
- Field, G. B. 1958, Proc. I.R.E., 46, 240
- Field, G. B. 1959, ApJ, 129, 551
- Fukugita, M., Hogan, C. J., & Peebles, P. J. E. 1998, ApJ, 503, 518
- Furlanetto, S., & Loeb, A. 2002, ApJ, submitted (astro-ph/0201313)
- Gnedin, N. Y. 2000, ApJ, 535, 530
- Gunn, J. E., & Peterson, B. A. 1965, ApJ, 142, 1633
- Haardt, F., & Madau, P. 1996, ApJ, 461, 20
- Haiman, Z. 2002, ApJ, submitted (astro-ph/0205410)
- Haiman, Z., Abel, T., & Madau, P. 2001, ApJ, 551, 599
- Haiman, Z., & Loeb, A. 1997, ApJ, 483, 21
- Haiman, Z., & Loeb, A. 1998, ApJ, 503, 505
- Hernquist, L., Katz, N., Weinberg, D., & Miralda-Escudé, J. 1996, ApJ, 457, L51
- Iliev, I. T., Shapiro, P. R., Ferrara, A., & Martel, H. 2002, ApJ, submitted (astro-ph/0202410)
- Kriss, G. A., et al.2001, Science, 293, 1112
- Mac Low, M.-M., & Ferrara, A. 1999, ApJ, 513, 142
- Madau, P., Ferrara, A., & Rees, M. J. 2001, ApJ, 555, 92
- Madau, P., Haardt, F., & Rees, M. J. 1999, ApJ, 514, 648
- Madau, P., Meiksin, A., Rees, M. J. 1997, ApJ, 475, 429
- Madau, P., & Rees, M. J. 2000, ApJ, 542, L69
- Meiksin, A., & Madau, P. 1993, ApJ, 412, 34
- Miralda-Escudé, J. 1998, ApJ, 501, 15
- Miralda-Escudé, J., Haehnelt, M., & Rees, M. J. 2000, ApJ, 530, 1
- Mori, M., Ferrara, A., & Madau, P. 2002, ApJ, 571, 40
- Purcell, E. M., & Field, G. B. 1956, ApJ, 124, 542
- Rauch, M., Sargent, W. L. W., & Barlow, T. A. 2001, ApJ, 554, 823
- Scannapieco, E., Ferrara, A., & Madau, P. 2002, ApJ, 574, 590
- Shapiro, P. R., Giroux, M. L. 1987, ApJ, 321, L107
- Shapiro, P. R., Giroux, M. L., & Babul, A. 1994, ApJ, 427, 25
- Shapiro, P. R., Raga, A. C., & Mellema, G. 1998, in Molecular Hydrogen in the Early Universe, Mem. Soc. Astr. It. 69, 463
- Shaver, P. A., Wall, J. V., Kellerman, K. I., Jackson, C. A., & Hawkins, M. R. S. 1996, Nature, 384, 439
- Shaver, P., Windhorst, R., Madau, P., & de Bruyn, G. 1999, A&A, 345, 380
- Songaila, A. 1997, ApJ, 490, L1
- Songaila, A. 2001, ApJ, 561, 153

- Steidel, C. C., Pettini, M., & Adelberger, K. L. 2001, ApJ, 546, 665
- Stern, D., Spinrad, H., Eisenhardt, P., Bunker, A. J., Dawson, S., Stanford, S. A., & Elston, R. 2000, ApJ, 533, L75
- Tegmark, M., Silk, J., & Evrard, A. 1993, ApJ, 417, 54
- Tozzi, P., Madau, P., Meiksin, A., & Rees, M. J. 2000, ApJ, 528, 59
- White, S. D. M., & Rees, M. J. 1978, MNRAS, 183, 341
- Zhang, Y., Anninos, P., & Norman, M. L. 1995, ApJ, 453, L57